Cell Reports
Report

Cell PRESS
Open ACCESS

Rhythmic Nucleotide Synthesis in the Liver: Temporal Segregation of Metabolites

Jean-Michel Fustin,[1] Masao Doi,[1] Hiroyuki Yamada,[1] Rie Komatsu,[1] Shigeki Shimba,[2] and Hitoshi Okamura[1,*]
[1]Department of System Biology, Graduate School of Pharmaceutical Sciences, Kyoto University, 46-29 Yoshida-Shimo-Adachi-cho, Sakyo-ku, Kyoto 606-8501, Japan
[2]Department of Health Science, College of Pharmacy, Nihon University, Funabashi, Chiba 274-8555, Japan
*Correspondence: okamurah@pharm.kyoto-u.ac.jp
DOI 10.1016/j.celrep.2012.03.001

SUMMARY

The synthesis of nucleotides in the body is centrally controlled by the liver, via salvage or de novo synthesis. We reveal a pervasive circadian influence on hepatic nucleotide metabolism, from rhythmic gene expression of rate-limiting enzymes to oscillating nucleotide metabolome in wild-type (WT) mice. Genetic disruption of the hepatic clock leads to aberrant expression of these enzymes, together with anomalous nucleotide rhythms, such as constant low levels of ATP with an excess in uric acid, the degradation product of purines. These results clearly demonstrate that the hepatic circadian clock orchestrates nucleotide synthesis and degradation. This circadian metabolome timetable, obtained using state-of-the-art capillary electrophoresis time-of-flight mass spectrometry, will guide further investigations in nucleotide metabolism-related disorders.

INTRODUCTION

The circadian clock synchronizes physiology and behavior to the appropriate time of day and endogenously generates rhythms under constant conditions. The clock regulates the transcription of thousands of target clock-controlled genes involved in fundamental metabolic pathways (Akhtar et al., 2002; Lamia et al., 2008; Panda et al., 2002; Reddy et al., 2006; Ueda et al., 2002; Vollmers et al., 2009), but the metabolic consequences of such regulation often remain to be described.

Two essential discoveries, the circadian control of the cell cycle (Matsuo et al., 2003) and DNA repair (Kang et al., 2010) in the liver, suggest the supply of nucleotides itself is regulated by the circadian clock. Since the liver is a site of active de novo nucleotide synthesis and controls the supply of free bases and nucleosides to other tissues for salvage (Barsotti et al., 2002; Cansev, 2006; Cao et al., 2005; Gasser et al., 1981), the circadian control of hepatic nucleotide metabolism will have wide implications for the body.

To define the role of the hepatic clock in the control of nucleotide metabolism, we analyzed gene expression and metabolome of wild-type (WT) and liver *Bmal1*-deficient mice (*Bmal1*$^{L-/-}$), which show rhythmic activity and food intake but lack a functional molecular clock in the liver driving hepatic physiology (Shimba et al., 2011). We show that the expression of rate-limiting enzymes in nucleotide metabolism is under clock control, and that nucleotides are rhythmic and time segregated. In *Bmal1*$^{L-/-}$ liver, aberrant expression of these enzymes is correlated with the disruption of nucleotide rhythms. In particular, ATP and was constantly low and uric acid was increased, suggesting inefficient purine synthesis and/or increased degradation. We here provide the first (to our knowledge) integrated transcriptome and metabolome circadian timetable focused on a single metabolic pathway, giving insights into the physiological importance of the local hepatic clock for nucleotide synthesis. This study is particularly relevant for cancer chemotherapy and for the treatment of nucleotide imbalance disorders such as gout.

RESULTS

The expression of genes involved in purine and pyrimidine nucleotide metabolism (KEGG mmu00230 and 00240, initially screened for rhythmic expression in microarray data set at http://circadian.salk.edu) was analyzed by quantitative real-time PCR from WT liver samples dissected every 4 hr during 24 hr. To avoid external interferences on the endogenous circadian clock, mice were housed in constant dark (DD) conditions with food and water ad libitum. To investigate the role of the liver circadian clock in the control of nucleotide biosynthesis, gene expression was analyzed in clock-less liver generated by liver-specific disruption of the clock gene *Bmal1* (Shimba et al., 2011). The loss of temporal hepatic organization was confirmed by the absence of *Bmal1* transcript and the aberrant rhythms of clock gene expression (Figure S1). For the sake of clarity, we report only genes that showed significant variations of expression ($p < 0.05$ in one-way ANOVA in WT). The results presented here are largely consistent with previous microarray data sets (Vollmers et al., 2009), but some genes showing very low-amplitude oscillations on microarray were not significant in our analysis.

Rate-Limiting Enzymes in De Novo Nucleotide Synthesis

De novo synthesis of nucleotides, with multiple enzymatic steps mediated by different genes, leads to the synthesis of inosine monophosphate (IMP, Figure 1A) or uridine monophosphate (UMP, Figure 1B), precursors for other nucleotides. The rate-limiting enzymes in the de novo synthesis of IMP (*Ppat*) (Nelson

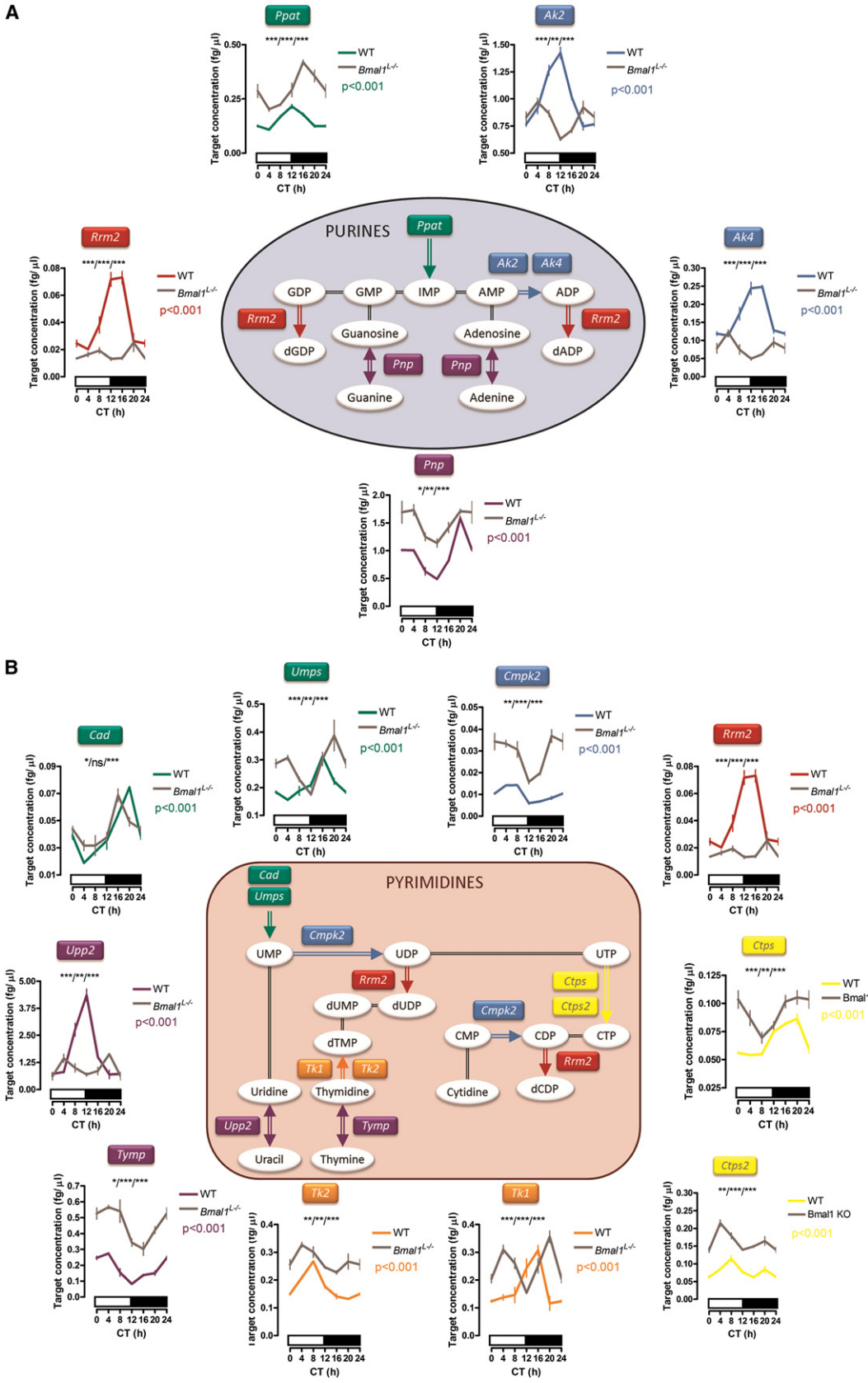
A
Ppat
Ak2
Rrm2
Ak4
Pnp
PURINES
GDP
GMP
IMP
AMP
ADP
dGDP
dADP
Guanosine
Adenosine
Guanine
Adenine
Target concentration (fg/ µl)
CT (h)
WT
Bmal1L-/-
p<0.001
B
Umps
Cmpk2
Cad
Upp2
Tymp
Tk2
Tk1
Ctps
Ctps2
PYRIMIDINES
UMP
UDP
UTP
dUMP
dUDP
dTMP
CMP
CDP
CTP
dCDP
Uridine
Thymidine
Cytidine
Uracil
Thymine
Bmal1
Bmal1 KO

et al., 2008) and UMP (*Cad* and *Umps*) (Traut, 2009; Traut and Jones, 1977) showed significant circadian rhythms of expression. In *Bmal1*$^{L-/-}$ liver, their expression was significantly affected (*Ppat* showing elevated levels) but still displayed a rhythmic component.

The de novo synthesis of CTP from UTP is mediated by two enzymes called CTP synthases. Two isoforms exist, *Ctps* (cytosolic) and *Ctps2* (mitochondrial), both mediating the rate-limiting step in the synthesis of cytidine nucleotides. *Ctps* expression was circadian but *Ctps2* showed significant bimodal variations. In *Bmal1*$^{L-/-}$ liver, both genes still displayed rhythmic expression with lower amplitude but with a 2-fold increase in baseline.

Together these data suggest the rhythmic de novo synthesis is under predominant systemic control, but modulated by the local liver clock.

Mitochondrial Nucleotide Monophosphate Kinases

The phosphorylation of nucleotide monophosphates, mediated by specific kinases, is a critical step toward the synthesis of NTPs (Nelson et al., 2008). Among these kinases, only the mitochondrial isoforms *Ak2*, *Ak4* (Figure 1A), and *Cmpk2* (Figure 1B) showed significant rhythmic expressions. *Ak2* and *Ak4* showed identical waveforms in WT and were similarly affected in *Bmal1*$^{L-/-}$, showing lower expression with a bimodal pattern. *Cmpk2* in contrast showed higher expression in *Bmal1*$^{L-/-}$ but remained rhythmic. This suggests that the rhythmic supply of nucleotide diphosphate, ADP in particular, is important in the mitochondria where ATP is synthesized. Lower *Ak* expression but higher *Cmpk2* expression may cause an imbalance in purine/pyrimidine content.

dNDP Synthesis Is Controlled by the Circadian Clock

Deoxynucleotide synthesis from nucleotide diphosphate is mediated by a single enzyme called ribonucleotide reductase M (RRM). RRM is composed of two subunits, RRM1 and RRM2 (Nelson et al., 2008), the latter being rate limiting for the activity of the enzyme (Zuckerman et al., 2011). *Rrm1* expression in liver was constant; while *Rrm2* displayed pronounced circadian variations (Figure 1; Figure S2B). Nadir *Rrm2* mRNA levels were three times lower than those of *Rrm1*, whereas at peak level they were equivalent, suggesting indeed a circadian control of RRM activity via regulation of *Rrm2* expression. In *Bmal1*$^{L-/-}$ liver, *Rrm2* remained constantly low. This particular enzyme is interesting since it operates both on purines and pyrimidines, and since the synthesis of dNTPs is specifically for DNA replication and repair. Lower *Rrm2* expression in clock-less liver may cause dNTPs insufficiency and hamper liver regeneration after injury.

Nucleotide Degradation and Salvage

The degradation of nucleosides to free bases, an important step for their subsequent salvage by other tissues (Balestri et al., 2007; Griffiths and Stratford, 1997; Markert, 1991; Pizzorno et al., 2002), is mediated by nucleoside phosphorylases. All hepatic nucleoside phosphorylases showed significant and high-amplitude rhythmic expression: *Pnp* (Figure 1A), *Tymp*, and *Upp2* (Figure 1B). *Pnp*, *Tymp*, and *Upp2* were highly expressed in the liver compared to other tissues (Figure S2A), but *Upp1* was barely detectable and was not significant (Figure S2B). In addition, *Tk1* and *Tk2*, salvaging thymidine to dTMP in the cytoplasm and mitochondria, respectively (Munch-Petersen, 2010), were rhythmically expressed in the liver (Figure 1B).

In *Bmal1*$^{L-/-}$ liver, *Upp2* expression lost its peak at CT12 and showed a low bimodal pattern. *Tymp* and *Pnp* showed increased expression, but with a residual rhythm of lower amplitude. *Tk1* and *Tk2* were both significantly affected, showing higher baseline and bimodal expression.

Together these results suggest that the hepatic clock, together with systemic cues, orchestrate nucleotide synthesis and degradation. To test this hypothesis, we quantified circadian liver metabolome by capillary electrophoresis time-of-flight mass spectrometry (CE-TOFMS) in WT mice, every 4 hr during 24 hr.

Rhythmic Abundance of Bases, Nucleosides, and Nucleotides by CE-TOFMS

CE-TOFMS analysis of liver metabolome revealed pervasive rhythms in free purine and pyrimidine bases, nucleosides, and nucleotides (Figures 2A and 2B).

The rhythms of IMP and UMP were similar to that of the expression of their own synthetic enzymes: *Ppat* and IMP rose during the day, *Cad* and *Umps* peaked at night with UMP.

The purine nucleotides ADP, ATP, GDP, and GTP all had similar phases (Figure 2A), which is consistent with the two parallel branches of the purine pathway. Since ATP allosterically regulates the synthesis of GMP from IMP, it is likely that the rhythm observed for ATP drives that of GTP. In contrast, all cytidine nucleotides showed significant bimodal patterns (Figure 2B), very similar to *Ctps2* expression. In contrast, UDP and UTP did not show significant variations.

Figure 1. Rate-Limiting Enzymes Are under Transcriptional Control by the Hepatic Circadian Clock

Gene expression analysis in C57BL/6J and *Bmal1*$^{L-/-}$ mice, on the second day in constant darkness, starting from CT0 (n = 3 mice per time points, sampled every 4 hr). One-way ANOVA was used to analyze gene expression profiles in WT mice, with significance levels given under the legend of each graph. Comparison of gene expression in the liver of C57BL/6J and *Bmal1*$^{L-/-}$ mice was performed by Two-way ANOVA, the significance levels are given under the title of each graph in the following order: interaction/genotype/time with *p < 0.05; **p < 0.01; ***p < 0.001. The empty and filled rectangles over the *x* axis indicate subjective day and night, respectively. For visual clarity, data at CT0 is double plotted at CT24 in all graphs.

(A) Gene expression analysis of enzymes in the purine pathway. A simplified purine metabolic pathway is shown in the center. Note the similar peak times for *Ppat*, *Rrm2*, *Ak2*, and *Ak4*, different from that of *Pnp*.

(B) Gene expression analysis of enzymes in the pyrimidine pathway. A simplified pyrimidine metabolic pathway is shown in the center. Green arrows indicate de novo synthesis (multiple enzymatic steps, but rate-limiting enzymes are indicated by a green label); blue, NMP kinases; red, NDP reductase; purple, nucleoside phosphorylases. Double black lines represent enzymatic activities encoded by nonrhythmic genes.

All data presented are mean ± SEM.

See also Figures S1, S2, and S4.

Cell PRESS
Open ACCESS

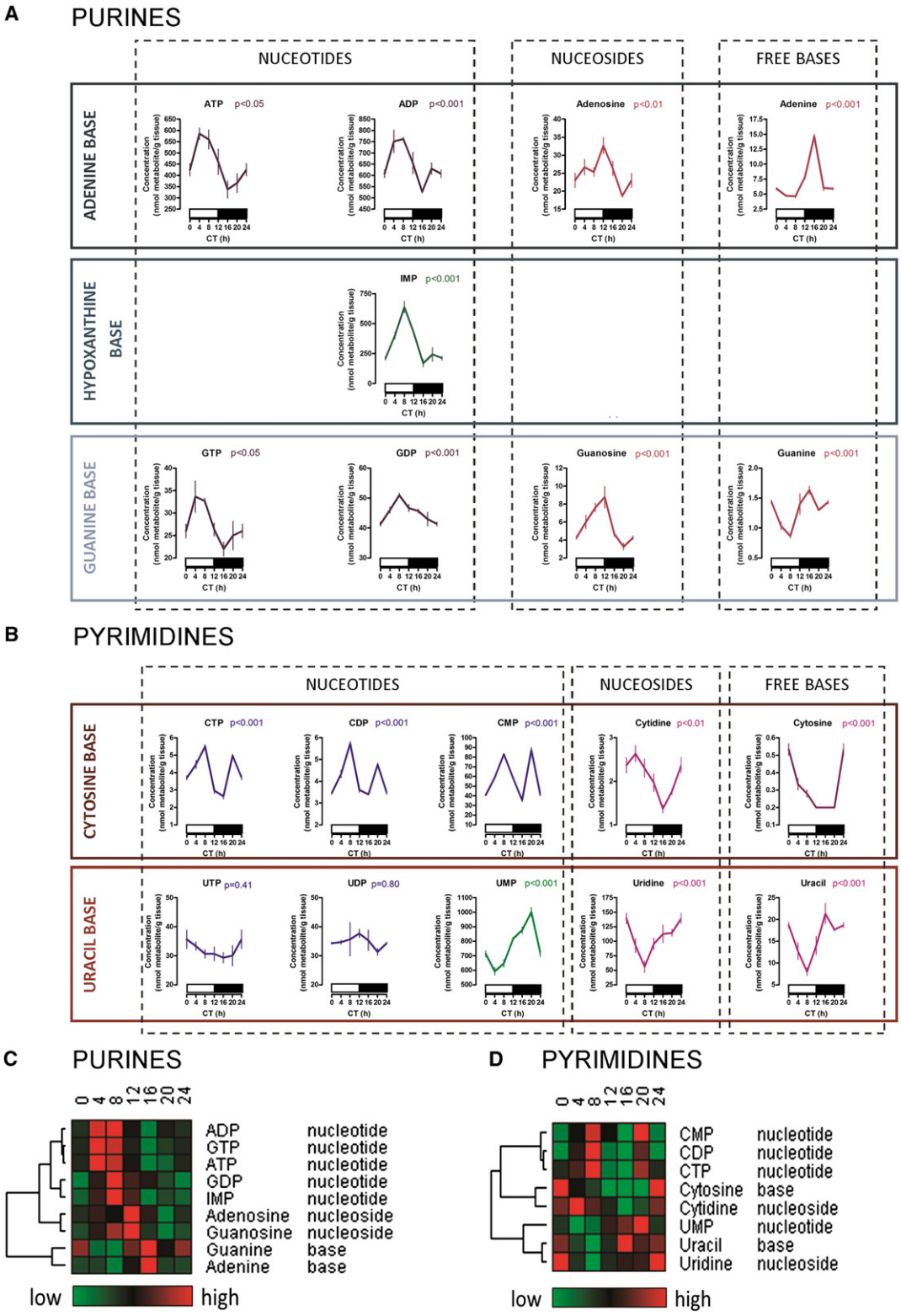

Figure 2. Rhythmic Abundance of Free Bases, Nucleosides, and Nucleotides in the Liver

Quantification of purine and pyrimidine nucleotides, nucleosides and free bases in the liver of C57BL/6J mice sampled on the second day in constant darkness from CT0 (n = 3 animals per time point). Significance levels in one-way ANOVA are given on the upper right corner of each graph. The empty and filled rectangles over the x axis indicate subjective day and night, respectively. Here, the color of curves indicates initial nucleotide monophosphate from the de novo pathway

The purine bases adenine and guanine peaked at night, rising at the end of the day in a pattern similar to *Pnp* expression and in antiphase to adenosine and guanosine. Similarly, uridine abundance was antiphasic to *Upp2* expression. Due to efficient degradation of pyrimidine free bases to soluble metabolites in the liver, the uracil rhythm closely mirrored that of uridine an order of magnitude lower. Since no cytidine phosphorylase has so far been discovered in mammals, it is likely that the rhythms observed for cytidine and cytosine depend mostly on digestion. A similar rhythm in cytidine, peaking during the subjective day, was previously reported in a partial circadian metabolomics study from mouse plasma (Minami et al., 2009).

Hierarchical clustering by Pearson correlation (Figure 2C) revealed that purines are time segregated, with nucleotides peaking in the mid-subjective day, followed by nucleosides at CT12, then by the adenine and guanine bases at CT16. ATP and GTP originate from the two opposite branches of the purine pathway but are perfectly synchronous. Clearly, a tight regulation of purines operates, resulting in a constant ratio between ATP and GTP throughout the day. Adenosine nucleotides are the most abundant purines (Figure S3A), reflecting their metabolic importance.

Hierarchical clustering of pyrimidines revealed a different pattern (Figure 2D). Here, the highest level of temporal organization reflected the nature of the base used, either uracil or cytosine. This underlines the differences between the two parallel and symmetric branches of the purine pathway versus the asymmetric and serial pyrimidine pathway (compare Figures 1A and 1B). The most abundant pyrimidine is UMP, consistent with it being the precursor for all other pyrimidine nucleotides (Figure S3B).

Similar to the disrupted rhythmic expression of genes presented in Figure 1, we predict that the nucleotide rhythms presented here will likewise be affected by the loss of the hepatic clock.

Loss of Liver Clock Affects Nucleotide Rhythms and Abundance

To determine which nucleotide rhythms and abundance are affected by the loss of the hepatic clock, we compared the nucleotide metabolome of *Bmal1*$^{L-/-}$ and *Bmal1*$^{f/f}$ mice at CT4 and CT16. These time points were chosen since they often correspond to high and low nucleotide abundance in WT mice. We present the results of this analysis organized in a metabolic map, similar to that used in Figure 1 (Figure 3).

IMP and UMP were little affected by the loss of the liver clock. While circadian time had a strongly significant effect on the abundance of both, only UMP showed a significant time/genotype interaction in two-way ANOVA. This is reminiscent of *Ppat*, *Cad*, and *Umps* expression in Figure 1: while they were affected by the loss of the hepatic clock, a rhythmic expression persisted, suggesting systemic control of de novo nucleotide synthesis by rhythmic cues.

AMP significantly increased in *Bmal1*$^{L-/-}$ liver but ATP remained low, which is consistent with the blunted expression pattern of *Ak2* and *Ak4*, resulting in a lower ADP/AMP ratio. The opposite branch of the purine pathway appeared similarly but somewhat less affected. GTP showed blunted CT4/CT16 fold ratio (genotype/time interaction significantly different in two way ANOVA, $p < 0.05$). Together this is consistent with a primary circadian regulation of ATP synthesis that in turn drives changes in GTP via allosteric control.

For pyrimidines, UTP and UDP were significantly lower in *Bmal1*$^{L-/-}$ liver, despite showing nonsignificant circadian variations in WT mice. CTP and CMP levels at CT4 were similar between genotypes, but at CT16 they increased in *Bmal1*$^{L-/-}$ liver while they decreased in WT, suggesting altered phase of synthesis, with higher basal synthesis level in clock-less liver.

The purine nucleosides adenosine and guanosine were less abundant in *Bmal1*$^{L-/-}$ liver, but showed CT4/CT16 variations as in WT. Adenine base however showed a reduction in the CT4/CT16 fold ratio. Low adenosine and blunted adenine rhythm are consistent with higher expression levels but lower amplitude rhythm observed for *Pnp* in Figure 1. For pyrimidine nucleosides, uridine showed increased levels in *Bmal1*$^{L-/-}$ liver, but cytidine was not affected.

Interestingly, the degradation product of purine nucleotides, uric acid, whose excess in human leads to gout, was elevated in *Bmal1*$^{L-/-}$ liver, suggesting indeed that the balance between synthesis (low ATP levels) and degradation (high urate) of purines is tilted toward degradation.

Together these data provide direct evidence that the hepatic circadian clock orchestrates the entire nucleotide metabolic pathway, in synchrony with systemic cues.

DISCUSSION

Nucleotide metabolism within the liver is orchestrated by the hepatic circadian clock but also synchronized at the level of the whole organism. First, de novo synthesis appears to respond mostly to systemic signals, which is consistent with the restricted feeding/fasting-driven rhythmic expression of *Ppat*, *Umps*, and *Cad* in clock-deficient animal reported in a previous data set (Vollmers et al., 2009). Second, the degradation of all nucleosides to their respective free bases appears regulated by the hepatic clock via control of phosphorylases transcription,

(green), NDP and NTP (blue) and free bases and nucleosides (purple), corresponding to the colors used for the enzyme activities contributing to the regulation of these metabolites. For visual clarity, data at CT0 are double plotted at CT24 in all graphs.

(A) Rhythmic profiles of purine nucleotides, nucleosides and free bases.

(B) Rhythmic profiles of pyrimidine nucleotides, nucleosides, and free bases.

(C) Hierarchical clustering of purines using Pearson correlation coefficient displayed as a heat map. Note the clear clustering between nucleotides, nucleosides and free bases, forming three separated time domains of maximal abundance.

(D) Hierarchical clustering of pyrimidines using Pearson correlation coefficient displayed as a heat map. Note here the clear higher-order clustering between cytidine nucleotides, nucleoside, and bases, and UMP, uridine, and uracil.

All data presented are mean ± SEM.

See also Figure S3.

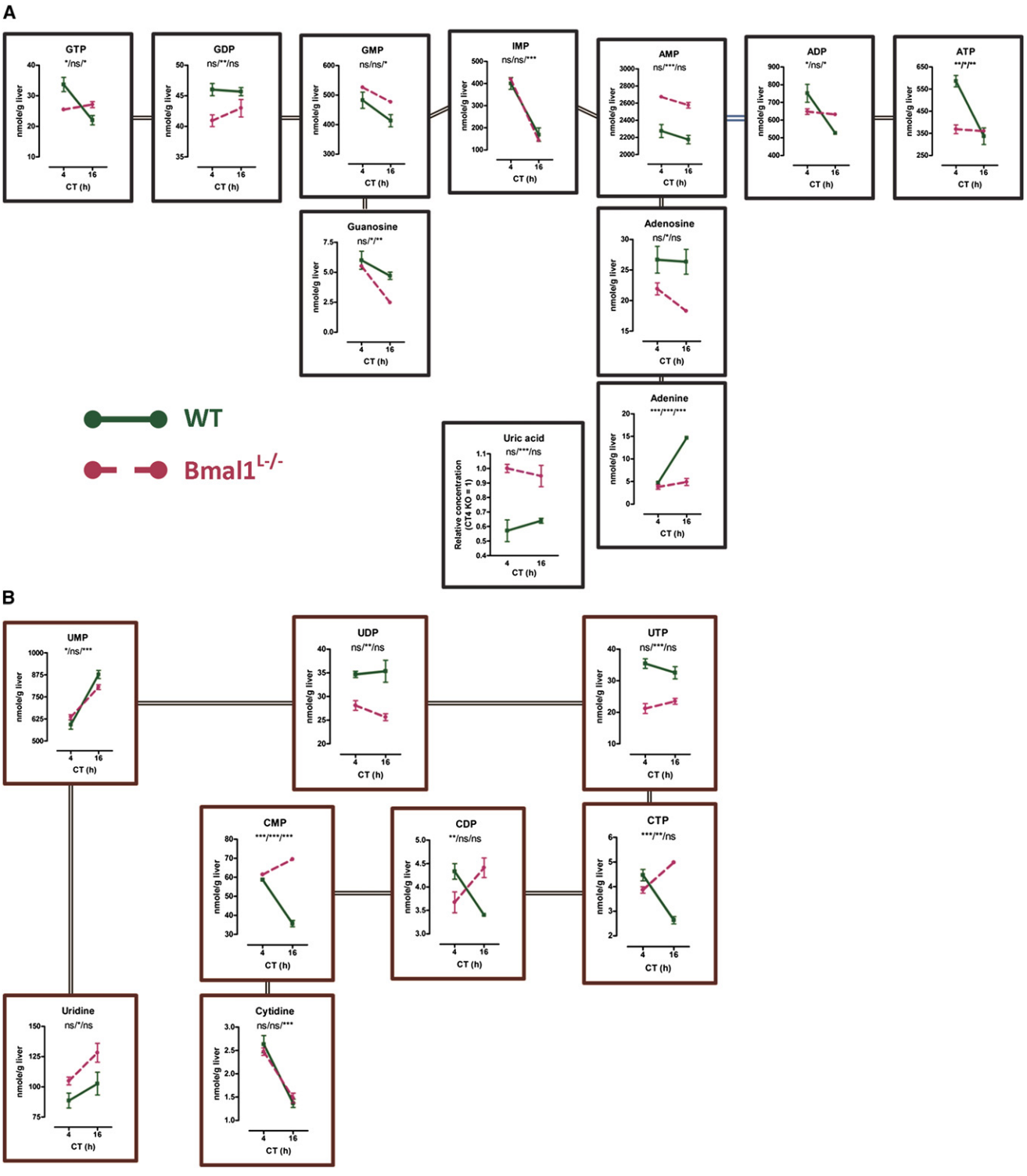

Figure 3. Loss of Liver Clock Affects Nucleotide Rhythms and Abundance

Absolute quantification of nucleotides, nucleosides and free bases in *Bmal1*$^{L-/-}$ and *Bmal1*$^{f/f}$ (WT) mice by CE-TOFMS at CT4 and CT16 (n = 2).

(A) Purine pathway. Note IMP rhythm persists in *Bmal1*$^{L-/-}$ liver while ATP remains low.

(B) Pyrimidine pathway. Note opposite changes in UTP and CTP. Data were analyzed by two-way ANOVA. Significance levels in two-way ANOVA are given under the title of each graph in the following order: interaction/genotype/time, with *p < 0.05; **p < 0.01; ***p < 0.001. All data presented are mean ± SD.

but the rhythmic abundance of nucleosides likely reflects their absorption from food. Indeed, all nucleoside variations between CT4 and CT16 show parallel changes in WT and clock-deficient liver. Taken together, systemic and local circadian regulation of nucleotide metabolism will regulate the amount of free bases and/or nucleosides released into the circulation for salvage, while ensuring an appropriately timed flow of newly synthesized nucleotides into the hepatic pool. This is especially obvious for purines, since all rhythmic genes involved in the anabolism of purines (*Ppat*, *Ak2*, *Ak4*, *and Rrm2*) show synchronized expression with a peak around CT12, in contrast to *Pnp* peaking at CT20.

The influence of the hepatic clock is mostly seen in the phosphorylation of nucleotides. All nucleotide triphosphates synthesized from their monophosphate forms (ATP, GTP, UTP) show lower abundance and/or amplitude in clock-less liver. The blunted *Ak2* and *Ak4* expression in *Bmal1*$^{L-/-}$ liver is consistent with these observations for ATP and GTP. UTP was not rhythmic in WT but its decreased abundance in *Bmal1*$^{L-/-}$ liver clearly indicates nucleotide synthesis as a whole suffers from the loss of the hepatic clock. The same is true for opposite variations of cytidine nucleotides.

The expression rhythms of mitochondrial kinases (*Ak2*, *Ak4*, *Cmpk2*, and *Tk2*) suggest that timed nucleotide conversion is especially important in mitochondria, perhaps because they rely exclusively on nucleotide salvage and have a more dynamic genome (Rötig and Poulton, 2009). Notably, AKs are critically important in the control of cellular energy homeostasis, by regulating the amount of ADP available for the synthesis of ATP (Noma, 2005), 70% of which originate from mitochondria. We propose that the constant low levels in *Ak2* and *Ak4* expression may contribute to decreased supply of ADP, in turn leading to low ATP levels, affecting, in turn, the synthesis of other nucleotides. Similarly, overexpression of both *Ctps* and *Ctps2* in *Bmal1*$^{L-/-}$ liver is likely to contribute to lower UTP and higher CTP and CMP levels observed in these animals.

Available data on the *Arabidopsis* circadian transcriptome (Mockler et al., 2007) reveal that plant homologs of *Rrm2*, *Ak*, *Ppat*, and *Cad* show a circadian component in their expression. Interestingly, most of these homologs are targeted to chloroplasts or mitochondria, where the de novo synthesis of nucleotides in plant is located (Zrenner et al., 2006). The evolutionary conserved circadian nucleotide synthesis, located in different subcellular compartments, essentially times maximal availability of nucleotides when they are required the most. As a concrete example in mammals, nucleotide excision repair activity in adult mouse liver and brain DNA is maximal at CT12 (Kang et al., 2009, 2010), when *Rrm2* expression is highest, replenishing the pool of dNTPs.

AMP-activated protein kinase (AMPK), whose activity is allosterically regulated by the AMP/ATP ratio, was found to regulate the circadian clock (Lamia et al., 2009). Interestingly, the AMP/ATP ratio will change during the day due to constant AMP levels but cyclic ATP abundance. The circadian clock thus regulates ATP levels, which may, in turn, feed back to adjust the clock in a complex interplay between metabolism and the clock, the topic of recent reviews (Asher and Schibler, 2011; Bass and Takahashi, 2010; Schmutz et al., 2011). The role of adenylate kinases, more precisely of *Ak2*, in the generation of circadian rhythms has even been suggested previously (Noma, 2005). To confirm the rhythmic expression of AK2, the variations of its protein in the liver are shown in Figure S4.

An important question that has not been addressed in our study is whether the disruption of nucleotide rhythms and abundance leads to pathologies in *Bmal1*$^{L-/-}$ animals. The increased uric acid observed in *Bmal1*$^{L-/-}$ liver, despite its efficient degradation in mouse liver (as opposed to human in which UOX, the enzyme oxidising urate, is a pseudogene), may have pathological consequences under special circumstances. In addition, the regenerating liver, as well as peripheral tissues with high proliferative rates such as bone marrow or thymus, may be adversely affected due to nucleotide imbalances seen in the liver of *Bmal1*$^{L-/-}$ animals. Further investigations will address these possibilities.

Conclusions

Hepatic nucleotide metabolism is timely orchestrated, from the transcriptional control of rate-limiting genes to the rhythmic abundance of metabolites. The loss of the local hepatic circadian clock causes significant perturbations in the normal rhythms of nucleotides, likely affecting the physiology of the whole animal. These results represent a novel integrative approach, linking transcriptomics with high-end metabolomics, focusing on the circadian control of a well-characterized metabolic pathway.

EXPERIMENTAL PROCEDURES

Animals

All experiments were approved by the animal experimentation committee of Kyoto University. Liver specific *Bmal1*-deficient mice on a full C57BL/6J background (*Bmal1*$^{L-/-}$) and *Bmal1*$^{f/f}$ were generated as described (Shimba et al., 2011). Male C57BL/6J mice and *Bmal1*$^{L-/-}$ mice (8 weeks old) were maintained at 23°C ± 1°C with 50% ± 10% relative humidity, three animals per cage on a 12-hr-light/12-hr-dark cycle (lights on 8:00, lights off 20:00), food and water ad libitum. At the end of the last dark phase, light was permanently switched off. On the second day in DD, starting from CT0 (CT0 beginning of the endogenous day, CT12 beginning of the endogenous night, 8:00 and 20:00, respectively), animals (n = 3) were sacrificed every 4 hr under a safe red light and sampled for liver RNA extraction and metabolomics analysis.

RNA Extraction and Quantitative Real-Time PCR

Mice were sacrificed by cervical dislocation and 50 mg from the left liver lobe were immediately transferred in 1ml Trizol (Invitrogen, Tokyo, Japan) and homogenized using TissueLyzer (QIAGEN, Tokyo, Japan). Homogenates were processed for total RNA extraction (RNeasy, QIAGEN), and final RNA samples were quantified by Nanodrop spectrophotometer. Total RNA (1.5 μg) from each liver sample was reverse-transcribed using VILO (Invitrogen). Quantitative real-time PCR was performed on 20 ng cDNA using Platinum SYBR Green qPCR Supermix (Invitrogen) in StepOnePlus (Applied Biosystems, Tokyo, Japan). Absolute quantification standards for each target cDNA were obtained using band-purified PCR products as templates, synthesized using the same primer pairs used in qPCR and verified by sequencing (see primer list in Table S1). All PCR products used for standard and quantification were of similar sizes (120–150 bp) and molecular weight (~40 kDa). Data were then normalized using relative expression of the housekeeping gene *Tbp*.

CE-TOFMS

At the time of liver sample collection for qPCR, another 50 mg sample from the left liver lobe, adjacent to the fragment previously taken, was excised and immediately transferred to a 2 ml tube, then snap-frozen in liquid nitrogen.

All samples were kept a few days at −80°C until analysis. Samples were then sent for CE-TOFMS analysis to Human Metabolome Technologies (Tokyo, Japan). See Supplemental Information for additional information.

Statistical Analyses

Gene expression and metabolites concentration in WT mice were analyzed by one-way ANOVA. To compare *Bmal1*$^{L-/-}$ and WT mice, gene expression profiles were tested by two-way ANOVA. All statistical analyses were performed using Graphpad Prism 4.0. For hierarchical clustering analysis of liver metabolites, raw concentration data of circadian metabolites were normalized and mean centered, and then clustered by Pearson correlation coefficients (Eisen et al., 1998). This was performed using GenePattern available from The Broad Institute.

SUPPLEMENTAL INFORMATION

Supplemental Information includes Extended Experimental Procedures, four figures, and one table and can be found with this article online at doi:10.1016/j.celrep.2012.03.001.

LICENSING INFORMATION

ACKNOWLEDGMENTS

This work was supported by Specially Promoted Research (to H.O.), and a scientific grant and the "High-Tech Research Center" Project for Private Universities, a matching fund subsidy (to S.S.) from the Ministry of Education, Culture, Sports, Science and Technology of Japan, and grants from the Health Labour Sciences Research of Japan, SRF, Takeda Science Foundation (to H.O.). J.-M.F. is supported by a JSPS Postdoctoral Fellowship Program (Short-term) for North American and European Researchers, a JSPS Postdoctoral Fellowship Program for Foreign Researchers and a Takeda Science Foundation research fellowship.

Received: October 18, 2011
Revised: February 13, 2012
Accepted: March 1, 2012
Published online: April 12, 2012

REFERENCES

Akhtar, R.A., Reddy, A.B., Maywood, E.S., Clayton, J.D., King, V.M., Smith, A.G., Gant, T.W., Hastings, M.H., and Kyriacou, C.P. (2002). Circadian cycling of the mouse liver transcriptome, as revealed by cDNA microarray, is driven by the suprachiasmatic nucleus. Curr. Biol. *12*, 540–550.

Asher, G., and Schibler, U. (2011). Crosstalk between components of circadian and metabolic cycles in mammals. Cell Metab. *13*, 125–137.

Balestri, F., Barsotti, C., Lutzemberger, L., Camici, M., and Ipata, P.L. (2007). Key role of uridine kinase and uridine phosphorylase in the homeostatic regulation of purine and pyrimidine salvage in brain. Neurochem. Int. *51*, 517–523.

Barsotti, C., Tozzi, M.G., and Ipata, P.L. (2002). Purine and pyrimidine salvage in whole rat brain. Utilization of ATP-derived ribose-1-phosphate and 5-phosphoribosyl-1-pyrophosphate generated in experiments with dialyzed cell-free extracts. J. Biol. Chem. *277*, 9865–9869.

Bass, J., and Takahashi, J.S. (2010). Circadian integration of metabolism and energetics. Science *330*, 1349–1354.

Cansev, M. (2006). Uridine and cytidine in the brain: their transport and utilization. Brain Res. Brain Res. Rev. *52*, 389–397.

Cao, D., Leffert, J.J., McCabe, J., Kim, B., and Pizzorno, G. (2005). Abnormalities in uridine homeostatic regulation and pyrimidine nucleotide metabolism as a consequence of the deletion of the uridine phosphorylase gene. J. Biol. Chem. *280*, 21169–21175.

Eisen, M.B., Spellman, P.T., Brown, P.O., and Botstein, D. (1998). Cluster analysis and display of genome-wide expression patterns. Proc. Natl. Acad. Sci. USA *95*, 14863–14868.

Gasser, T., Moyer, J.D., and Handschumacher, R.E. (1981). Novel single-pass exchange of circulating uridine in rat liver. Science *213*, 777–778.

Griffiths, L., and Stratford, I.J. (1997). Platelet-derived endothelial cell growth factor thymidine phosphorylase in tumour growth and response to therapy. Br. J. Cancer *76*, 689–693.

Kang, T.H., Reardon, J.T., Kemp, M., and Sancar, A. (2009). Circadian oscillation of nucleotide excision repair in mammalian brain. Proc. Natl. Acad. Sci. USA *106*, 2864–2867.

Kang, T.H., Lindsey-Boltz, L.A., Reardon, J.T., and Sancar, A. (2010). Circadian control of XPA and excision repair of cisplatin-DNA damage by cryptochrome and HERC2 ubiquitin ligase. Proc. Natl. Acad. Sci. USA *107*, 4890–4895.

Lamia, K.A., Storch, K.F., and Weitz, C.J. (2008). Physiological significance of a peripheral tissue circadian clock. Proc. Natl. Acad. Sci. USA *105*, 15172–15177.

Lamia, K.A., Sachdeva, U.M., DiTacchio, L., Williams, E.C., Alvarez, J.G., Egan, D.F., Vasquez, D.S., Juguilon, H., Panda, S., Shaw, R.J., et al. (2009). AMPK regulates the circadian clock by cryptochrome phosphorylation and degradation. Science *326*, 437–440.

Markert, M.L. (1991). Purine nucleoside phosphorylase deficiency. Immunodefic. Rev. *3*, 45–81.

Matsuo, T., Yamaguchi, S., Mitsui, S., Emi, A., Shimoda, F., and Okamura, H. (2003). Control mechanism of the circadian clock for timing of cell division in vivo. Science *302*, 255–259.

Minami, Y., Kasukawa, T., Kakazu, Y., Iigo, M., Sugimoto, M., Ikeda, S., Yasui, A., van der Horst, G.T., Soga, T., and Ueda, H.R. (2009). Measurement of internal body time by blood metabolomics. Proc. Natl. Acad. Sci. USA *106*, 9890–9895.

Mockler, T.C., Michael, T.P., Priest, H.D., Shen, R., Sullivan, C.M., Givan, S.A., McEntee, C., Kay, S.A., and Chory, J. (2007). The DIURNAL project: DIURNAL and circadian expression profiling, model-based pattern matching, and promoter analysis. Cold Spring Harb. Symp. Quant. Biol. *72*, 353–363.

Munch-Petersen, B. (2010). Enzymatic regulation of cytosolic thymidine kinase 1 and mitochondrial thymidine kinase 2: a mini review. Nucleosides Nucleotides Nucleic Acids *29*, 363–369.

Nelson, D.L., Cox, M.M., Lehninger, A.L., and Lehninger, A.L. (2008). Lehninger Principles of Biochemistry (New York: Freeman).

Noma, T. (2005). Dynamics of nucleotide metabolism as a supporter of life phenomena. J. Med. Invest. *52*, 127–136.

Panda, S., Antoch, M.P., Miller, B.H., Su, A.I., Schook, A.B., Straume, M., Schultz, P.G., Kay, S.A., Takahashi, J.S., and Hogenesch, J.B. (2002). Coordinated transcription of key pathways in the mouse by the circadian clock. Cell *109*, 307–320.

Pizzorno, G., Cao, D., Leffert, J.J., Russell, R.L., Zhang, D., and Handschumacher, R.E. (2002). Homeostatic control of uridine and the role of uridine phosphorylase: a biological and clinical update. Biochim. Biophys. Acta *1587*, 133–144.

Reddy, A.B., Karp, N.A., Maywood, E.S., Sage, E.A., Deery, M., O'Neill, J.S., Wong, G.K., Chesham, J., Odell, M., Lilley, K.S., et al. (2006). Circadian orchestration of the hepatic proteome. Curr. Biol. *16*, 1107–1115.

Rötig, A., and Poulton, J. (2009). Genetic causes of mitochondrial DNA depletion in humans. Biochim. Biophys. Acta *1792*, 1103–1108.

Schmutz, I., Albrecht, U., and Ripperger, J.A. (2011). The role of clock genes and rhythmicity in the liver. Mol. Cell. Endocrinol. *349*, 38–44.

Shimba, S., Ogawa, T., Hitosugi, S., Ichihashi, Y., Nakadaira, Y., Kobayashi, M., Tezuka, M., Kosuge, Y., Ishige, K., Ito, Y., et al. (2011). Deficient of a clock

gene, brain and muscle Arnt-like protein-1 (*BMAL1*), induces dyslipidemia and ectopic fat formation. PLoS ONE *6*, e25231.

Traut, T. (2009). Nucleotide Synthesis *De Novo* (Chichester, UK: John Wiley & Sons Ltd).

Traut, T.W., and Jones, M.E. (1977). Inhibitors of orotate phosphoribosyltransferase and orotidine-5′-phosphate decarboxylase from mouse Ehrlich ascites cells: a procedure for analyzing the inhibition of a multi-enzyme complex. Biochem. Pharmacol. *26*, 2291–2296.

Ueda, H.R., Chen, W., Adachi, A., Wakamatsu, H., Hayashi, S., Takasugi, T., Nagano, M., Nakahama, K., Suzuki, Y., Sugano, S., et al. (2002). A transcription factor response element for gene expression during circadian night. Nature *418*, 534–539.

Vollmers, C., Gill, S., DiTacchio, L., Pulivarthy, S.R., Le, H.D., and Panda, S. (2009). Time of feeding and the intrinsic circadian clock drive rhythms in hepatic gene expression. Proc. Natl. Acad. Sci. USA *106*, 21453–21458.

Zrenner, R., Stitt, M., Sonnewald, U., and Boldt, R. (2006). Pyrimidine and purine biosynthesis and degradation in plants. Annu. Rev. Plant Biol. *57*, 805–836.

Zuckerman, J.E., Hsueh, T., Koya, R.C., Davis, M.E., and Ribas, A. (2011). siRNA knockdown of ribonucleotide reductase inhibits melanoma cell line proliferation alone or synergistically with temozolomide. J. Invest. Dermatol. *131*, 453–460.